Uncertainties in Estimating Turbulent Fluxes to Melting Snow in a Mountain Clearing

WARREN D. HELGASON[1] AND JOHN W. POMEROY[1]

ABSTRACT:

The turbulent fluxes of heat and water vapour were studied in a 7.5 ha clearing in Marmot Creek Research Basin, located in the Kananaskis River Basin in the Rocky Mountains of Alberta, Canada. A locally homogeneous site surrounded by forested mountainous terrain was instrumented allowing 5-level profile measurements of wind speed, temperature, and water vapour, as well as two levels of eddy covariance measurement. Mean profiles exhibit logarithmic distribution with height up to 2.5 m height. The momentum roughness length values, z_{0m} derived from the eddy covariance measurements were at least an order of magnitude larger than typical values over snow, indicating that the air flow was much more turbulent than would be expected from shear stress developed at the snow surface. Accordingly, the measured wind profile did not match to the expected wind profile using Monin-Obukhov similarity theory and first-order closure methods. Despite this discordance, the increased turbulence appears to be well matched to the temperature and water vapour profiles, confirming the measured latent and sensible heat fluxes. Gravimetric evaporation measurements provided further agreement with the latent heat flux measured by the eddy covariance technique. The failure of Monin-Obukhov similarity theory at this site suggests that the application of flux estimation techniques that are based on flux-profile relationships would predict smaller heat flux values than those that were measured.

Keywords: snowmelt, eddy correlation/covariance, sensible heat, flux-profile, latent heat, sublimation, Rocky Mountains

INTRODUCTION

In western Canada, a large proportion of the surface water supply is derived from seasonal mountain snowpacks. The timing, intensity and duration of Rocky Mountain snowmelt are of great interest in streamflow calculations for the Saskatchewan-Nelson river system. However there are longstanding concerns about substantial evaporation of Rocky Mountain snowpacks, particularly during highly convective 'chinook' wind events (Storr, 1967, Golding, 1978). Besides reducing via vaporization the snow mass available for melt, the turbulent fluxes of sensible heat and water vapour and associated latent heat exchange are important for calculations of snowmelt rate. The relative importance of turbulent energy sources for snowmelt varies markedly with timing of snowmelt and geographical location (Male and Gray, 1981; Morris, 1989). For example, at an alpine site in the Rocky Mountains Cline (1995), attributed 25% of the seasonal snowmelt energy to turbulent sources, while at a Canadian prairie site, Pomeroy et al. (1998) found the turbulent contribution to melt of a continuous snowcover to be insignificant in most conditions. Pomeroy et al. (2003) showed that the relative magnitude and direction of the sensible heat flux to melting

[1] Centre for Hydrology, University of Saskatchewan, 117 Science Place, Saskatoon, Saskatchewan S7N 5C8 Canada.

snow can vary markedly within a small mountain catchment due to insolation, slope, aspect, and vegetation exposure.

Turbulent fluxes over snow surfaces can be measured directly using the Eddy Covariance technique (eg. Munro, 1989; Smeets et al., 1998; Box and Steffen, 2001; Arck and Sherer, 2002; Andreas et al., 2005). However, the specialized instrumentation required to use the eddy covariance technique is not always available, and other estimation techniques must then be utilized. The most popular of these are the semi-empirical flux-profile relationships that relate heat and vapour fluxes to measured temperature and humidity gradients and a convection term. The most commonly applied flux-profile relationships are the bulk transfer method (eg. Moore, 1983; Kondo and Yamazawa, 1986) and the aerodynamic profile method (eg. Munro and Davies, 1978; Hood et al., 1999; Denby and Snellen, 2002). The utility of both the direct eddy covariance measurement and flux-profile estimation techniques are limited to the range in which their underlying assumptions are valid. Generally the flux-profile estimates are considered more sensitive to violations of the constant vertical flux layer and horizontal steady state assumptions behind the technique. However, even eddy covariance assumes that the 'footprint' observed by the sonic anemometer is a homogenous surface and that the properties of the air flow vary slowly (Gash, 1986). In contrast, mountain environments sustain complex and highly variable air flows over heterogeneous surfaces. Despite this discord between the assumptions of turbulent transfer relationships, Monin-Obukhov theory and the actual characteristics of airflow in mountains, there is great interest in using eddy correlation measurement and/or flux-profile estimation techniques in areas exhibiting local homogeneity, such as forest stands, alpine meadows, and forest clearings. This paper examines the measurement uncertainty in applying eddy covariance and flux profile relationships in locally homogeneous forest clearing in the mountains.

METHODS

Study Site

The study site is located in the Marmot Creek Research Basin (50º 56' N, 115º 08' W) situated in the Kananaskis river basin in the eastern slopes of the Rocky Mountains, Alberta, Canada. The measurement tower was erected in the "Hay Meadow" (Figure 1); a relatively large (7.3 ha) clearing in the valley bottom. The Hay Meadow site gently slopes at an average grade of 2.5% southeast, is covered by short grasses (<20 cm tall) and is surrounded by mixed aspen and spruce forest, in which the trees are approximately 13 m tall. A small row of aspen trees located south of the measurement tower location limits the unobstructed upwind fetch to between 35 and 135 m depending on the direction of the wind.

At the valley bottom daily average temperatures vary from –7°C in December and January to 14°C in July and August. Cold winter temperatures are frequently alleviated by "chinook" (foehn) winds that transport warm and very dry Pacific air into the region resulting in rapid increases in temperatures to values well above 0°C. Precipitation received in the Kananaskis River Valley is approximately 600 mm of which approximately 70% is snowfall.

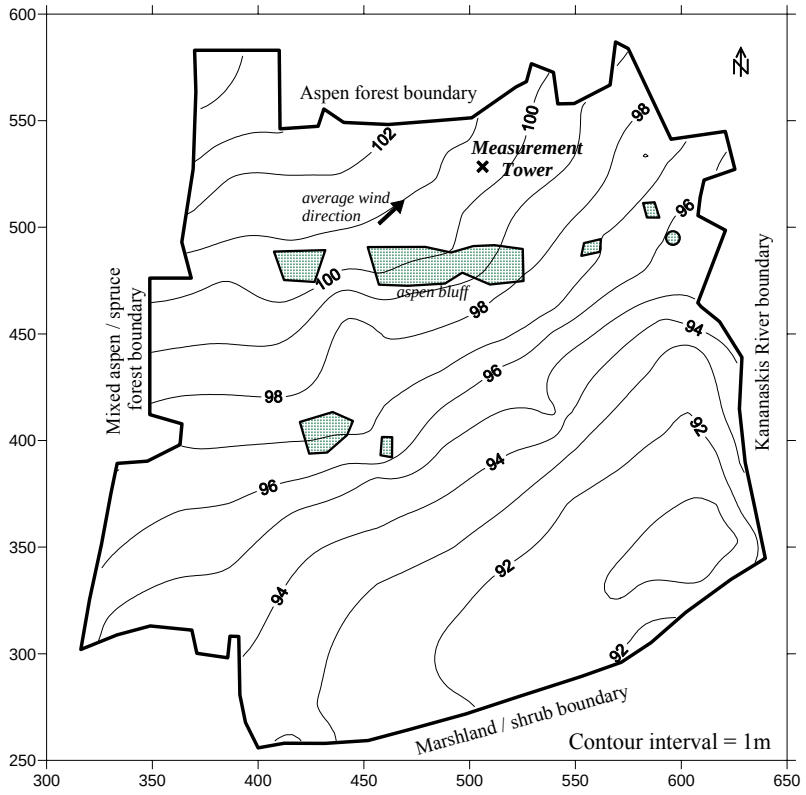

Figure 1. "Hay Meadow" clearing

Instrumentation

A 5m tower was erected in November, 2004 and then instrumented as described below in January, 2005. The tower and instrumentation as installed can be seen in Figure 2.

The fluxes of heat, vapour and momentum were measured using 2 eddy covariance systems mounted at 1.95 m and 3.80 m above the ground surface. Each system consisted of a "Campbell Scientific CSAT3" 3-dimensional sonic anemometer and a "Campbell Scientific KH20 Hygrometer" to measure the water vapour fluctuations. The sensors were sampled at 10 Hz, from which average means, variances, and co-variances were computed at 15 min. intervals.

Measurements of the temperature profile were made at 5 heights (0.40, 1.23, 2.39, 3.54, and 4.45 m above ground) using 0.076 mm diameter, E-type thermocouples. "Vaisala HMP45C212 Hygrothermometers" were installed at the same heights to measure the water vapour profile, as well as allowing for a redundant temperature profile. The hygrothermometers were installed in naturally-aspirated 12-plate "Gill" radiation shields. Prior to installation, the hygrometers were cross-referenced by installing all of the sensors in a mechanically-ventilated enclosure and allowing the temperature and humidity to vary over the expected range. Calibration equations were then developed to adjust the response of each probe to that of an arbitrarily-selected reference probe. This procedure was necessary to overcome the small differences in factory calibration between the sensors and to allow them to be used for profile measurements.

Additional wind speed and direction measurements were made using "Met One 50.5" 2-dimensional sonic anemometers mounted at heights of 1.23, 2.39, and 4.40 m above ground, which correspond to 3 of the heights of the temperature and humidity profiles. These instruments were programmed to sample the wind speed at 10 Hz, and then return a average value from the

past one second when polled by the datalogger. In order to minimize the obstruction of wind flow near the tower these sensors were placed on an auxiliary mast that extended off of the main tower.

Auxiliary measurements included incoming and outgoing short- and long-wave radiation using "Kipp and Zonen CNR1" and snow depth using a "Campbell Scientific Canada SR50" ultrasonic depth sensor. This information was used to calculate the actual height of the instruments with respect to the snow surface for each time period. All of the sensors were recorded using 2 "Campbell Scientific CR23X" dataloggers and one "CR10X" datalogger. All sensors, except for the eddy covariance instruments, were polled at 5-sec. intervals, and then the resulting statistical parameters were output on 15-min intervals.

Eddy Covariance Technique

The eddy covariance method employs fast response sensors to measure the rapid fluctuations of wind velocity, temperature and water vapour. The wind velocity components in the x, y, and z directions are noted as u, v, and w respectively, where u is the stream-wise velocity, v is span-wise velocity and w is the velocity normal to the plane of flow. In this experiment the right-handed coordinate system is established with respect to the alignment of the head of the sonic anemometer, which was pointed due South and aligned parallel to the gently sloping surface.

The momentum flux, τ can then be found as in (1) from the covariance of wind velocity components in the vertical and horizontal directions. Similarly the heat flux, H or water vapour flux, E is calculated in (2) and (3) from the covariance of fluctuations of the vertical wind velocity and potential temperature, θ or vapour content, q. Values presented with an overbar represent time averaged means, whereas the fluctuating part is represented by a prime superscript. The symbol ρ represents the atmospheric density and c_p, the specific heat capacity of the atmosphere.

$$\tau = -\rho\sqrt{\left(\overline{u'w'}\right)^2 + \left(\overline{v'w'}\right)^2} \quad (1)$$

$$H = \rho c_p \overline{w'\theta'} \quad (2)$$

$$E = \rho\overline{w'q'} \quad (3)$$

In addition to the three fluxes previously mentioned, the sonic anemometer provides important information on the flow at the measurement point. The degree of atmospheric stability, ζ which is the ratio of the height, z to the Obhukov length, L can be found by (4), where u^* is the friction velocity defined in (5), T_a is the average virtual temperature, g is gravitational acceleration, and k is the von Kármán constant taken as 0.4.

$$L = -\frac{u^{*3} T_a \rho c_p}{kgH} \quad (4)$$

$$u^* = \sqrt{\frac{\tau}{\rho}} \quad (5)$$

The results presented here deal primarily with the lower level of turbulence measurements. However, development of the surface layer to the height of the upper system was verified by checking for similar fluxes and turbulence characteristics at both heights.

Gravimetric Measurements of Evaporation

Direct measurements of snow evaporation were made using simple lysimeters. Three white plastic containers with a surface area of approximately 900 cm^3, and a depth of 7 cm were filled with an undisturbed snow sample, and then placed into a cavity created in the snowpack such that the lip of the container was level with the surrounding snow. The snow surface at the interface was then recreated as realistically as possible. Each morning of the study, the containers were weighed and then they were refilled with snow excavated nearby and replaced in the snowpack. The average reduction mass of the three contrainers was then used to calculate the evaporation loss from the snowpack.

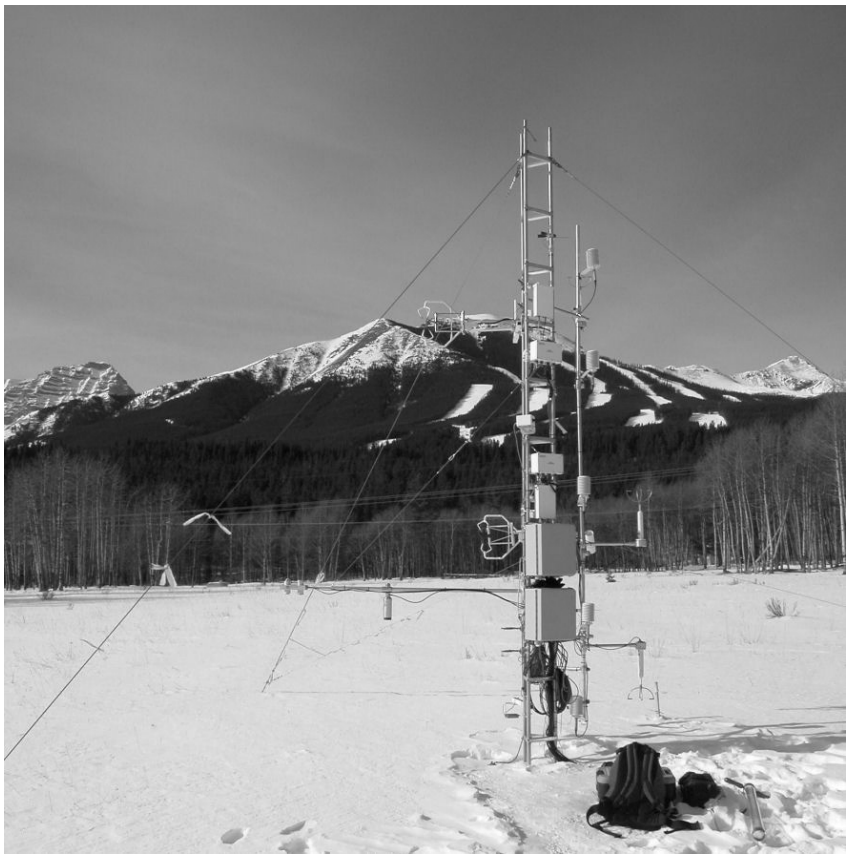

Figure 2. Instrument tower (view from the East).

Flux Gradient Relationships

In many hydrology studies, the high frequency instrumentation required to make direct measurements of the turbulent fluxes are not available. Instead, methods that relate the turbulent covariances to mean variables are employed. The most common method used is based on eddy diffusivity theory, which suggests that the turbulent flux of momentum stress, or some other scalar, is proportional to the gradient of the entity being transferred. This relationship is presented in (6) and (7) for the momentum flux, where K_m is the eddy diffusivity for momentum. Similar expressions are used to replace the covariances in (2) and (3) with K_h and K_v respectively.

$$\tau = K_m \rho \frac{\partial \overline{u}}{\partial t} \quad (6)$$

$$K_m = ku * z \quad (7)$$

The mean wind, temperature, and vapour gradients can be measured between two heights or between a reference height and the ground surface. Expressions (8) to (10) illustrate the latter case, where the subscript s denotes the snow surface value, z_{0m}, z_{0v}, and z_{0h} are the roughness lengths for momentum, vapour, and heat, while Ψ is the stability correction.

$$\overline{q}_s - \overline{q} = \frac{E}{k u_* \rho}\left[\ln\left(\frac{z}{z_{0v}}\right) - \Psi_v(\zeta)\right] \qquad (8)$$

$$\overline{\theta}_s - \overline{\theta} = \frac{H}{k u_* \rho c_p}\left[\ln\left(\frac{z}{z_{0h}}\right) - \Psi_h(\zeta)\right] \qquad (9)$$

$$\overline{u} = \frac{u_*}{k}\left[\ln\left(\frac{z}{z_{0m}}\right) - \Psi_m(\zeta)\right] \qquad (10)$$

The stability corrections employed for stable conditions were simple linear functions where $\psi_m = 5.8\zeta$, and $\psi_h = 5.4\zeta$ (Cheng and Brutsaert, 2005). For unstable cases, the stability corrections of Paulson (1970) were used. Note that z_{0v}, and z_{0h} are typically much smaller than that for momentum.

RESULTS

Data Selection

The data selected for presentation in this paper is from Feb. 24, through Mar 3, 2005. The weather at the site was reasonably consistent during this period. The days and evenings were mainly clear, and air temperatures ranged from –10 C during the evening to +10C during the day. The net solar radiation balance was positive during the day and negative during the evening. Snow depth as measured with the ultrasonic sensor was 10 cm on Feb 24th, and had ablated to 8 cm by Mar. 3rd. The snow cover was initially uniform, but then developed small bare patches during the last few days of the period. This was reflected in the daytime albedo values calculated from the incoming and outgoing shortwave radiation values that decreased over the period from an initial value of 0.77 to 0.54. The winds were light during the evening and increased during the day, but the 15-min. mean values always remained below 3.5 m s^{-1}. At this sire, winds are typically experienced as short gusts, rather than sustained flows. Winds were predominantly from of the southwest (Figure 1).

Mean Profiles

Sample profiles of mean hourly wind speed, temperature, and specific humidity collected on March 2 are shown in Figure 3. The wind profiles (Figure 3a) have been have been plotted as separate series' according to the type of anemometer used. Generally, at wind speeds greater than 1.0 m s^{-1} the 2-D (Met-One 50.5) sonic anemometers reported values that differed from the 3-D (Campbell Scientific CSAT3) sonic anemometers. In addition to the offset observed in Figure 3, occasionally one of the 2-D anemometers would report a sporadic value that was inconsistent with the overall wind profile provided by the rest of the instruments. The observed inconsistency made it difficult to distinguish disturbances in the wind profile from apparently erroneous sensor readings. All of the anemometers installed at the site were new and had been subject to recent factory calibrations. The 3-D anemometers provided more reliable wind measurements and are believed to be more accurate. This is attributed to the more sophisticated internal signal processing and self-diagnostic features of the CSAT3 sensor, as well as the authors' previous experience with these instruments and previous intercomparisons with other sonic, cup and propeller based anemometers. Overall, the information provided by the wind profiles is somewhat uncertain due to the inconsistencies introduced by the two types of sonic anemometers.

The mean temperature and vapour profiles typically exhibited logarithmic behaviour in the lowest 2.5 m or more of the atmosphere. However, during afternoons, the observations of temperature and water vapour at 3.5 m and above deviated from the expected logarithmic profile. This departure reveals some type of perturbation that is likely an artefact of the surrounding complex terrain.

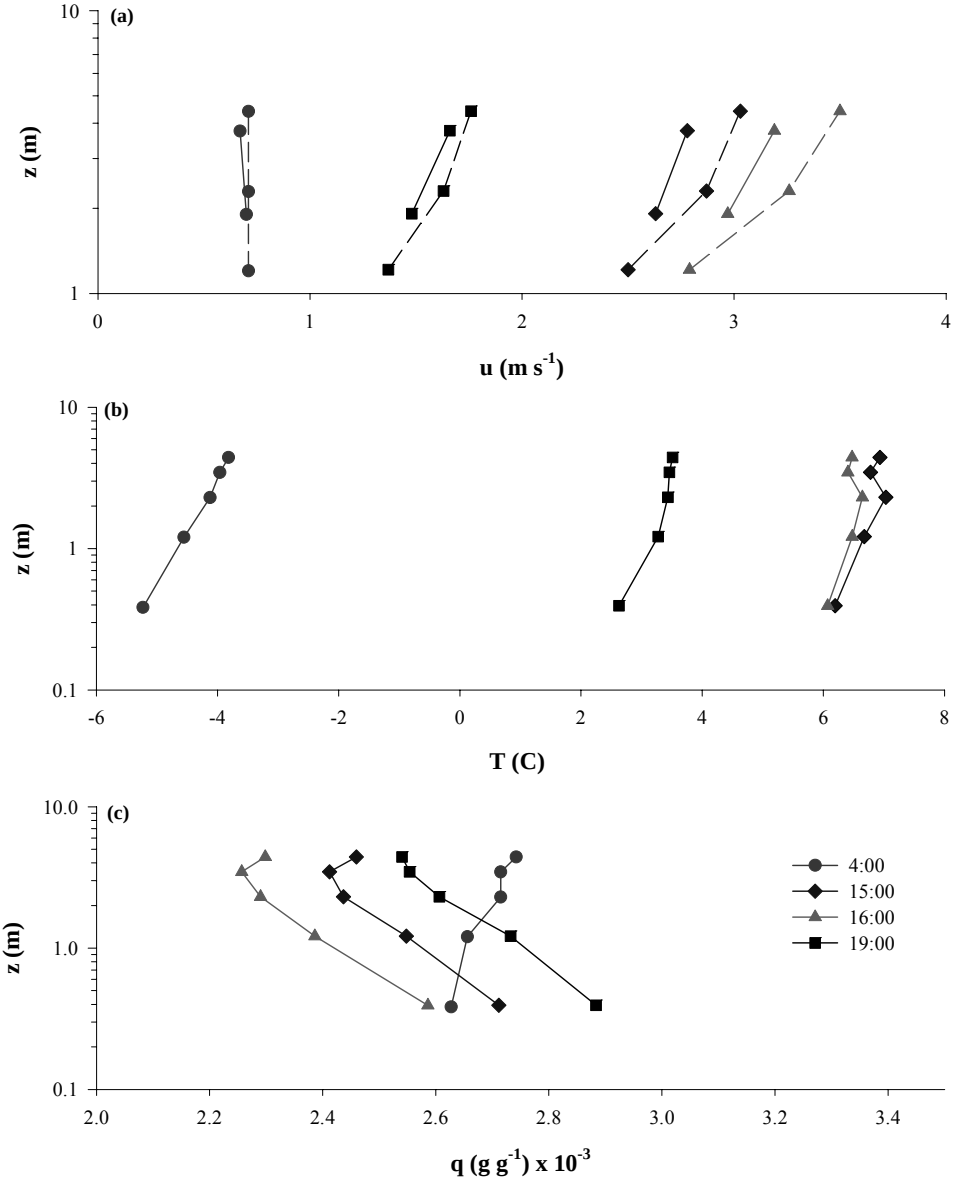

Figure 3. Sample 1-hr mean profiles of wind (a), temperature (b), and water vapour (c) collected on March 2, 2005. The dashed lines in (a) are mean winds measured with the Campbell Scientific CSAT3 , whereas the continuous lines are measured with the Met One 50.5.

Measured Fluxes

Eddy Covariance Fluxes

The hourly-averaged heat fluxes measured by the eddy covariance method are presented in Figure 4. The latent heat flux exhibited a typical diurnal cycle with peak daily values of 45 W m^{-2}. Negative latent heat flux values indicate condensation, which did occur on some early mornings (confirmed by water vapour profile slopes). The sensible heat flux exhibited greater scatter than the latent heat flux values. Most of the values were negative, indicating that heat energy was being transferred from the air to the snowpack.

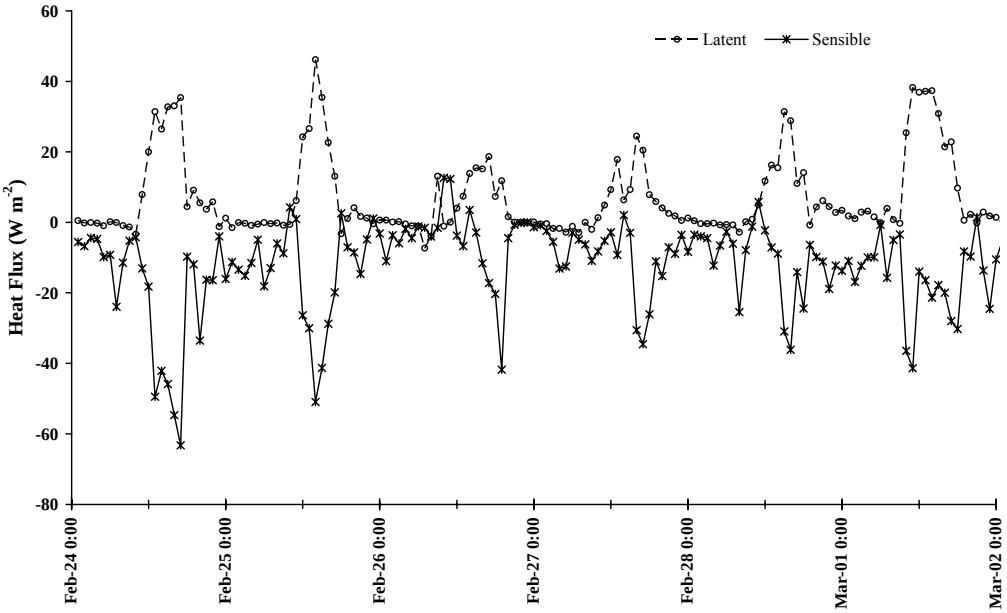

Figure 4. Hourly heat fluxes measured using eddy covariance technique at 1.95 m

Lysimeter Evaporation

The daily evaporation amounts measured with the lysimeter pans are presented in Figure 5, where they are compared to those measured by the eddy covariance method. It is possible that the sides of the plastic lysimeter pan may have heated up due to solar radiation penetration through adjacent snow and then provided extra energy to the snow within the pan. This may contribute to why the evaporation measured by the lysimeter was greater than the eddy covariance measurement on four of the days. The largest discrepancies occurred on Feb 26th and 27th. These days both correspond to small fluxes measured by the eddy covariance method (Figure 4). On Feb 26th the lysimeter measured a net mass gain that may be attributed to a large condensation event. Condensation can not be accurately measured with the KH20 hygrometer as the sensor becomes coated with ice, and signal quality degrades. Overall, the agreement indicated in Figure 5 suggests that the fluxes measured by the eddy covariance technique are representing the actual conditions.

Flow Characterization

Atmospheric Stability

The values of ζ obtained from (4) indicate that conditions were neutral ($-0.0625<\zeta<0.125$) for 80% of the 192 hourly periods that were examined. The remaining hours were mildly stable ($\zeta <$ 0.75) in early morning with a relatively few unstable periods in the afternoon.

Surface roughness parameterization

In atmospheric flows, the ability of the surface roughness to absorb momentum is often represented by the momentum roughness length, z_{0m}. Accordingly, in well developed flows where turbulence is primarily caused by shear at the surface, the roughness length becomes an appropriate parameter to express the development of turbulence. By rearranging (10) and solving for z_{0m}, where $\overline{u}$ is measured from the 3-D sonic anemometer at 1.95 m above ground, the average momentum roughness length was z_{0m} = 0.18 m. This measurement at least one order of magnitude larger than other values reported for snow surfaces. Moore (1983) summarizes z_{0m} values reported over snow, and reports that most smooth snow surfaces are in the range of 1.0 x 10^{-3} m and rough surfaces around 5.0 x 10^{-3} m. Andreas et al. (2005) present a roughness length formulation for snow-covered sea ice that is based on friction velocity. For the range of u^* values measured in this study, the values predicted by the Andreas et al. (2005) model should lie in the range of 1.0 x 10^{-4} to 1.0 x 10^{-3} m. This large difference between the measured z_{0m} values and the expected values indicates that the flow was not in equilibrium with the local snow surface.

Another method of estimating z_{0m} values is to plot ln(z) vs. $\overline{u}$ for neutral conditions and then determine the value of z_{0m} as the y-intercept where $\overline{u}$ =0. This procedure, when applied to the mean wind speeds measured by the 3-D sonic anemometers provided an average z_{0m} value of 7.0x10^{-3} m. This value is in close agreement to what is expected for flow over a snow surface. These results suggest that the mean wind profile was in equilibrium with the snow surface, however the turbulence was not.

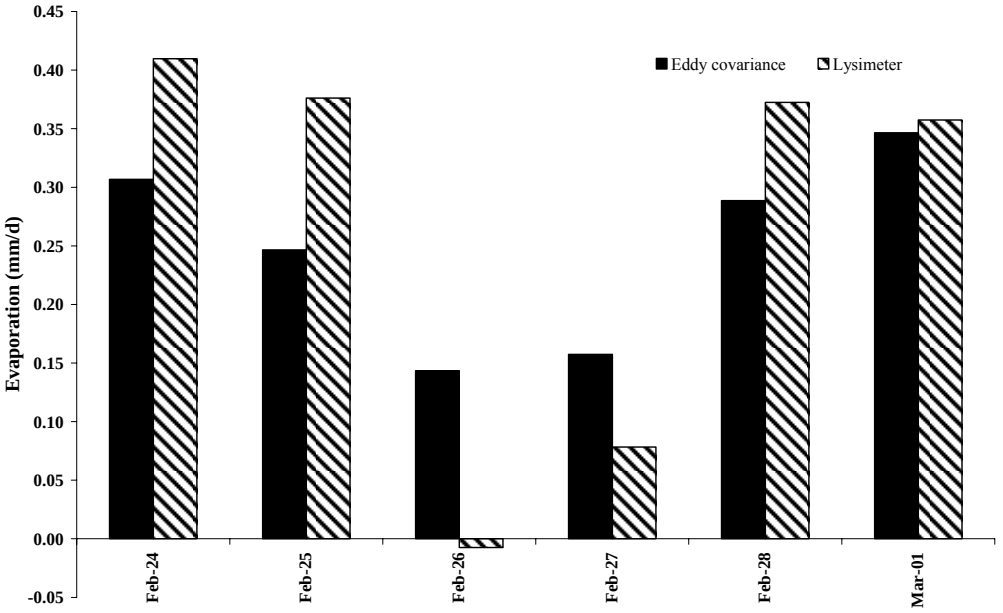

Figure 5. Daily snow sublimation measured with snow lysimeter and eddy covariance technique.

Deduced Profiles from Measured Parameters

Figure 6 presents the theoretical vertical profiles of wind speed, potential temperature and specific humidity that should result from the measured turbulent fluxes. Equations (8) to (10) were used to predict the expected value at each measurement height based on the values of E, H, and u* along with the roughness lengths determined from the eddy covariance system. In the case of the wind profiles (Figure 6a) the predicted gradient is much steeper than the measured value. This suggests that the momentum fluxes measured from eddy covariance were not only due to the friction of the local snow surface, but may include additional turbulence due to complex upstream wind flow.

The temperature and water vapour profiles (Figure 6b,c) were well matched to the expected values calculated from the eddy covariance observations. This suggests that the measured value of u* is realistic, even though it was much larger than what the local smooth snow surface would be capable of generating.

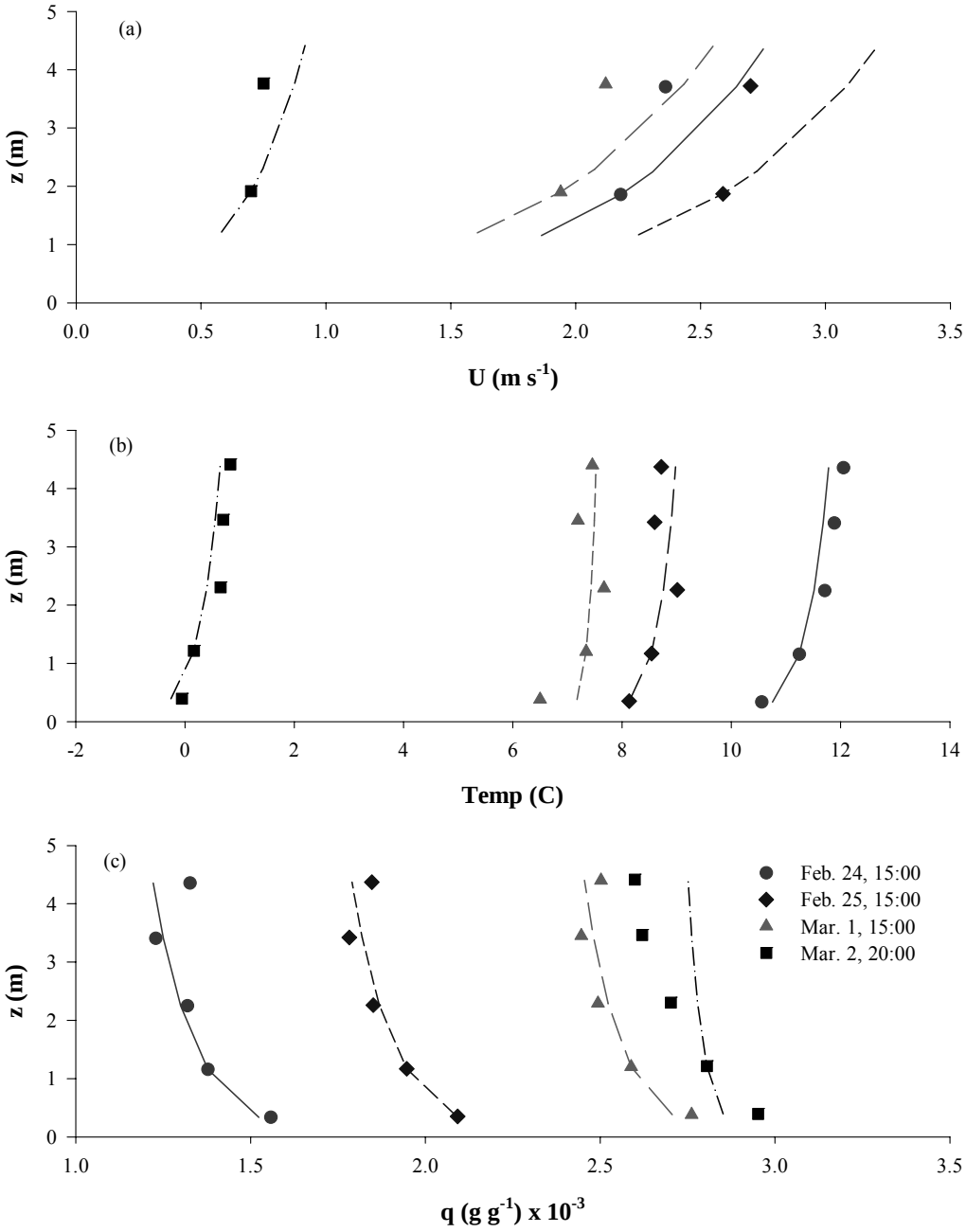

Figure 6. Fitting measured profile data to flux-profile curves for (a) wind speed, (b) temperature, and (c) water vapour. Lines indicate theoretical profiles based on Monin-Obuhkov similarity theory driven by eddy covariance measurements, points are observations from anemometers, thermocouples and hygrometers.

Turbulence Characteristics

Standard deviations, σ of the wind velocity components were calculated from the variances measured by the eddy covariance technique. When normalized by dividing by u*, these relationships are referred to as the integral turbulence characteristics. In neutral and unstable atmospheric conditions, the values of $\sigma_u/u*$, $\sigma_v/u*$, and $\sigma_w/u*$, can be estimated using Monin-Obukhov similarity theory when measured over homogeneous terrain (Panofsky and Dutton, 1984). However, in non-homogeneous or complex terrain, the horizontal variances often differ from the predicted values due to the slow adjustment of large horizontal eddies to surface roughness changes (eg. Beljaars, 1987). Measurements from near neutral conditions as well as some typical values reported by (Panofsky and Dutton, 1984) are presented in Table 1. Due to the blocking effect of the surface, the largest eddy size represented in the vertical wind variance is on the order of the height of the wind speed sensor. Eddies of this size are capable of adjusting quite quickly to changes in surface roughness. However, the horizontal variance is made up of much larger eddies that may have length scales of several hundred metres (Panofsky et al., 1978). These large eddies adjust much slower to surface changes, and correspondingly retain some of the behaviour of the upstream roughness characteristics. The observed ratios of vertical variance to friction velocity show near typical values at the 3.8 m height but smaller values below. The lower values at 1.95 m may be due to unresolved fast eddies or they indicate the need for coordinate rotation at this height. The observed ratios of horizontal variance to friction velocity show values that are typical of mountain terrain rather than level terrain, suggesting that a 'memory' of turbulence from the surrounding mountains affects turbulence in the level clearing.

Table 1. Integral turbulence characteristics (mean values in parentheses). Measured values for 1.95 and 3.80 m height and typical values provided by Panofsky and Dutton (1984) for level and mountain sites.

	$\sigma_w/u*$	$\sigma_{hor}/u*$
Measured: z = 1.95m	0.97	3.85–4.37
Measured: z = 3.80m	1.20	4.25–4.51
Typical: Level terrain	1.10–1.40 (1.25)	1.8–2.5 (2.15)
Typical: Mountain terrain	1.24	3.8–4.5 (4.15)

DISCUSSION

The high value of z_{0m} obtained under neutral conditions at this site suggests that the air flow is much more turbulent (and indicative of greater terrain roughness) than one would expect given the smooth nature of the snow surface and the small wind speed gradients that were measured. Consequently, the measured fluxes of sensible and latent heat are higher than would be predicted by estimation techniques that are based on Monin-Obukhov similarity theory and textbook values of roughness lengths. Previous studies have indicated that the shear stress due to the snow surface results in z_{0m} values that are one to two orders of magnitude smaller than those measured in this study. This suggests that the measured turbulence was not in equilibrium with the local surface, yet in this case measured turbulence controlled the measured heat and vapour fluxes. As the mean wind speed profiles were adjusted to the snow surface roughness, whereas the turbulence was not, the link between the Reynolds stress and the mean gradients could not be described through first order turbulence closure. As a result, the flux-profile technique is not appropriate for estimating turbulent fluxes for snowmelt at this location.

The integral turbulence characteristics indicate that large horizontal eddies contribute to the large horizontal wind variances present at this site. Applying the hypothesis of Townsend (1961), these large scale motions have often been thought to be a source of inactive turbulence (eg. Beljaars, 1987). However, measurements by Andreas (1987) and Smeets *et al*. (1998) suggest that topographically induced low frequency motions do in-fact affect the cospectra of momentum, as

well as scalar transport. Högström *et al*. (2002) and McNaughton *et al*. (2002) also challenge Townsend's hypothesis regarding inactive turbulence.

The clearing chosen for this study is relatively homogeneous for a mountain environment and represents a site where there is great need to understand melt rates and the effect of forest clearing on the same. Although the fetch lengths reported in this study and the integral turbulence characteristics should be acceptable for eddy covariance studies (Gash, 1986) if not flux-profile, it is important to realize that fetch distances greater than 50 m are rare in the environments that are of importance to mountain hydrology and so the uncertainty in flux estimation found here may be quite common in mountain snow hydrology studies. Flux estimation for snowmelt calculations in these environments will require knowledge of local topographic influences on turbulence and the recognition that local scale turbulence in a clearing is also influence by the surrounding terrain.

CONCLUSIONS

Whether the source of the extra turbulence is due to the upstream roughness from forests or to large scale turbulence associated with mountain roughness, it is clear that turbulent fluxes of sensible and latent heat from small mountain forest clearings cannot be estimated through first-order closure theories, such as the eddy diffusivity theory and flux-gradient relationships. This calls into question the use of bulk transfer theory in these environments without the use of effective roughness parameters. In contrast, direct flux measurement using eddy covariance resulted in water vapour fluxes that were consistent with surface evaporation measurements, suggesting that the more relaxed assumptions behind employment of eddy covariance systems can permit their use for snowmelt studies in mountain environments. Turbulent fluxes in the mountain clearing were larger than would be estimated by classical flux profile methods with standard roughness lengths for snow. Further work is required to ascertain whether bulk transfer relationships can be applied reliably in such environments.

ACKNOWLEDGEMENTS

The authors would like to acknowledge the expert contribution of Michael Solohub, Centre for Hydrology, University of Saskatchewan in all aspects of the field study. Logistical support was provided by the Kananaskis Field Station, University of Calgary. The study was supported financially by an NSERC Discovery Grant and the Canada Research Chair in Water Resources and Climate Change with equipment provided by grants from the Canada Foundation for Innovation, NSERC and the Province of Saskatchewan Science and Technology Fund.

REFERENCES

Andreas EL. 1987. Spectral measurements in a disturbed boundary layer over snow. *Journal of the Atmospheric Sciences* **44**(15): 1912–1939.

Andreas EL, Jordan ER, Makshtas AP. 2005. Parameterizing turbulent exchange over sea ice: the Ice Station Weddell results. *Boundary-Layer Meteorology* **114**: 439–460.

Arck M, Scherer D. 2002. Problems in the determination of sensible heat flux over snow. *Geografiska Annaler: Series A, Physical Geography* **84**(3–4): 157–169.

Beljaars ACM. 1987. On the memory of wind standard deviation for upstream roughness. *Boundary-Layer Meteorology* **38**: 95–101.

Box JE, Steffen K. 2001. Sublimation on the Greenland ice sheet from automated weather station observations. *Journal of Geophysical Research* **106(D24)**: 33,965–33,981.

Cheng Y ,Brutsaert W. 2005. Flux-profile relationships for wind speed and temperature in the stable atmospheric boundary layer. *Boundary-Layer Meteorology* **114**: 519–538.

Cline D. 1995. Snow surface energy exchanges and snowmelt at a continental alpine site. *In* Biogeochemistry of Seasonally Snow-covered Catchments, Tonnessen K, Williams MW, Tranter M (eds.). IAHS Publication no. 228. IAHS Scince: Boulder CO; 156–166.

Denby B, Snellen H. 2002. A comparison of surface renewal theory with the observed roughness length for temperature on a melting glacier surface. *Boundary-Layer Meteorology* 103: 459–468.

Garratt JR. 1990. The internal boundary layer – a review. *Boundary-Layer Meteorology* **50**: 171–203.

Gash, J. 1986. Observations of turbulence downwind of a forest-heath interface. *Boundary-Layer Meteorology* **36**: 227–237

Golding, DL 1978. Calculated snowpack evaporation during chinooks along the eastern slopes of the Rocky Mountains in Alberta. *Journal of Applied Meteorology* **17(11)**: 1647–1651.

Golding DL, Swanson RH. 1978. Snow accumulation and melt in small forest openings in Alberta. *Canadian Journal of Forest Research* **8**: 380–388.

Male DH, Gray DM. 1981. Snowcover ablation and runoff. *In* Handbook of Snow: Principles, Processes, Management & Use, Gray DM, Male DH (eds.). Pergamon Press: Toronto; 776.

Högström U, Hunt JCR, Smedman AS. 2002. Theory and measurements for turbulence spectra and variances in the atmospheric neutral surface layer. *Boundary-Layer Meteorology* **103**: 101–124.

Hood EM, Williams M, Cline D. 1999. Sublimation from a seasonal snowpack at a continental mid-latitude alpine site. *Hydrological Processes* **13**: 1781–1797.

Kaimal JC, Finnigan JJ. 1994. Atmospheric Boundary Layer Flows: Their Structure and Measurement. Oxford University Press: Oxford; 289.

Kondo J, Yamazawa H. 1986. Bulk transfer coefficient over a snow surface. *Boundary-Layer Meteorology* **34**: 123–135.

McNaughton KG, Brunet Y. 2002. Townsend's hypothesis, coherent structures and Monin-Obukhov similarity. *Boundary-Layer Meteorology* **102**: 161–175.

Moore RD. 1983. On the use of bulk aerodynamic formulae over melting snow. *Nordic Hydrology* **14(4)**: 193–206.

Morris EM. 1989. Turbulent transfer over snow and ice. *Journal of Hydrology* **105**: 205–223.

Munro DS. 1989. Surface roughness and bulk heat transfer on a glacier: comparison with eddy correlation. *Journal of Glaciology* **34(121)**: 343–348.

Munro DS, Davies JA. 1978. On fitting the log-linear model to wind speed and temperature profiles over a melting glacier. *Boundary-Layer Meteorology* **15**: 423–437.

Panofsky HA, Egolf CA, Lipschutz R. 1978. On characteristics of wind direction fluctuations in the surface layer. *Boundary-Layer Meteorology* **15**: 439–446.

Panofsky HA, Dutton JA. 1984. Atmospheric Turbulence: Models and Methods for Engineering Applications. John Wiley & Sons: New York; 397.

Paulson CA. 1970. The mathematical representation of wind speed and temperature profiles in the unstable atmospheric surface layer. *Journal of Applied Meteorology* **9**: 857–861.

Pomeroy JW, Toth B, Granger RJ, Hedstrom NR, Essery RLH. 2003. Variation in surface energetics during snowmelt in a subarctic mountain catchment. *Journal of Hydrometeorology* **4**: 702–719.

Pomeroy W, Gray DW, Shook K, Toth B, Essery R, Pietroniro A, Hedstrom N. 1998. An evaluation of snow accumulation and ablation processes for land surface modelling. *Hydrological Processes* **12**: 2339–2367.

Smeets CJPP, Duynekerke PG, Vugts HF. 1998. Turbulence characteristics of the stable boundary layer over a mid-latitude glacier. Part 1: a combination of katabatic and large-scale forcing. *Boundary-Layer Meteorology* **87**: 117–145.

Storr, D. 1967. Precipitation variations in a small forested watershed. In *Proceedings of 35th Western Snow Conference*: 11–17.

Townsend AA. 1961. Equilibrium layers and wall turbulence. *Journal of Fluid Mechanics* **11**: 97–120.